The sapphirine-bearing rocks in contact with the Lherz peridotite body: new mineralogical data, age and interpretation

Supplementary Material

SM1: Operating conditions for the LA-ICP-MS equipment

Laboratory & Sample Preparation	
Laboratory name	Géosciences Rennes, UMR CNRS 6118, Rennes, France
Sample type/mineral	Rutile in thin sections
Sample preparation	In context in thin sections
Imaging	BSE images were acquired using a JEOL JSM-IT300 SEM
Laser ablation system	
Make, Model & type	ESI NWR193UC, Excimer
Ablation cell	ESI NWR TwoVol2
Laser wavelength	193 nm
Pulse width	< 5 ns
Fluence	7 J/cm2
Repetition rate	5 Hz
Spot size	35 µm
Sampling mode / pattern	Single spot
Carrier gas	100% He, Ar make-up gas and N2 (3 ml/mn) combined using in-house smoothing device
Background collection	20 seconds
Ablation duration	60 seconds
Wash-out delay	15 seconds
Cell carrier gas flow (He)	0.76 l/min
ICP-MS Instrument	
Make, Model & type	Agilent 7700x, Q-ICP-MS
Sample introduction	Via conventional tubing
RF power	1350W
Sampler, skimmer cones	Ni
Extraction lenses	X type
Make-up gas flow (Ar)	0.85 l/min
Detection system	Single collector secondary electron multiplier
Data acquisition protocol	Time-resolved analysis
Scanning mode	Peak hopping, one point per peak
Detector mode	Pulse counting, dead time correction applied, and analog mode when signal intensity > ~ 10^6 cps
Masses measured	^{204}(Hg + Pb), ^{206}Pb, ^{207}Pb, ^{208}Pb, ^{232}Th, ^{238}U
Integration time per peak	10-30 ms
Sensitivity / Efficiency	20000 cps/ppm Pb (50µm, 10Hz)
Data Processing	
Gas blank	20 seconds on-peak
Calibration strategy	R10 primary reference material, R19 secondary reference material (quality control)
Reference Material info	R10 and R19 (Zack et al., 2011)
Data processing package used	Iolite (Paton et al., 2010), VizualAge_UcomPbine (Chew et al., 2014)
Quality control / Validation	R19: intercept age = 495 ± 5.4 Ma (N=8; MSWD=0.64)

SM2: Thin section descriptions

1. Momo 1

At the macroscopic scale, this sample appears as a friable orange-brown sandstone. A layering is defined by a grain-size sorting with alternating greenish to greyish, silt-sized to sand-sized millimetric beds of isolated broken minerals and polymineralic debris deriving from different lithologies. The polymineralic debris are subangular to rounded. The monomineralic clasts are all angular. Polymineralic clasts include: unserpentinized and serpentinized ultramafic rocks, meta-ophite, as well as one clast of enstatite-gabbro and one of granitic gneiss. Ultramafic clasts are either composed of olivine and enstatite (sometimes with chromian hercynite) or of enstatite and diopside. These associations correspond respectively to harzburgite and to websterite. Due to their small size, the clasts are not necessarily directly representatives of their protoliths. Therefore, it cannot be proved here that massive pyroxenites furnished debris to the Lherz breccias unlike what is reported for the content of breccia deposits on top of the Lherz body (Lagabrielle & Bodinier, 2008). Meta-ophitic clasts are made up of plagioclase (An22.7–22.8) and magnesio-hornblende, sometimes with clinopyroxene. A single clast composed of olivine, plagioclase (An56.9–58.10) and enstatite was observed. This clast could either derive from a Cretaceous alkaline enstatite-gabbro as known in the Aulus Basin (Les Plagnaux gabbro, Montigny *et al*., 1986; Ternet *et al*., 1997) or from the cumulate portion of an ophitic intrusion (Azambre *et al.*, 1987). A last polymineralic clast-type consists of quartz, phlogopite and muscovite and shows a foliation, suggesting a derivation from an orthogneiss. Isolated detritial minerals include: magnesio-hornblende, enstatite, chromian hercynite, phlogopite, muscovite, clinopyroxene, quartz, chlorite and several types of plagioclase (An18 to An58). Most of the plagioclases are extremely rich in inclusions such as green hornblende, apatite and fluid inclusions.

2. Momo 2a

Momo 2a was sampled in the whitest part of the outcrop. This poorly consolidated rock gleaming in the sun contains phyllites sizing up to 2 centimetres in a white cement. Under the microscope, this rock appears as a coarse-grained sandstone made of monomineralic clasts of dominant vermiculite cemented by euhedral calcite. In some parts of the thin section, calcite crystals reach a millimetric size. The vermiculites are often grouped in bouquets or in clusters of parallel crystals. There is no clear fabric at the scale of the thin section. The vermiculite crystals are always kinked with cleavages coated by oxides and with frequent voids between bent crystal lamellae. The edges are diffuse, often with ponytail aspects. Vermiculite seems to derive from the transformation of a former phyllite (likely a phlogopite). Sparse and strongly fractured pargasite and gedrite are scattered within the thin section. The very high content in isolated crystals of vermiculite does not correspond to a classical metamorphic protolith and is better explained by a sedimentary overconcentration.

3. Momo 2b

This white rock was sampled at a distance of 50 centimetres from Momo 2a sample, in the same light coloured and shiny unit. At the macroscopic scale, it shows a layering interrupted by discontinuities resembling microfaults. At the microscopic scale, Momo 2b sample is a microbreccia with millimetric to submillimetric monomineralic clasts cemented by euhedral calcite. Isolated minerals include: dominant vermiculite, sapphirine, aluminous spinel, magnesio-hornblende, gedrite and apatite. The phyllites often display a yellowish to greenish pleochroism and are kinked, with opened cleavages and often with ponytail edges. Interstratified chlorites-vermiculites correspond to the most coloured greenish-yellowish species. The layering and the fault-like discontinuities are underlined by the alignment of the vermiculite flakes. Like in Momo 2a sample, the microclasts are all strongly fractured with opened fractures filled by calcite.

4. LHZ 49

This layered orange-brown fine-grained sandstone is exposed ten metres above the Momo 2a and 2b white sandstones. It is exclusively made up of angular, submillimetric monomineralic clasts from a dominant ultramafic protolith. Clasts include: olivine (89.9 – 91% forsterite), diopside, enstatite, Ti-pargasite, hercynite, chromian hercynite, chlorite and minor quartz. Planar minerals are roughly parallel-oriented, thus defining a coarse bedding.

5. BCOR 71

At a macroscopic scale, this sample has an overall light brown colour and is dotted by multiple white spots. Beige layers with submillimetric white spots alternate with brown layers with more numerous millimetric white spots. The brown colour corresponds to an accumulation of intertwined small and highly pleochroic phlogopites. The beige colour reflects lower concentrations in phlogopite. The white spots are scapolite crystals, usually isolated but sometimes grouped in two or three specimens. In both kinds of layers, the thin section is predominantly made of a tight association of granular diopside crystals with intergrowths of small phlogopites. A few occurrences of epidote (allanite) and tourmaline (uvite) crystals are reported. The scapolite crystals often display a poikiloblastic texture, with fine grained inclusions of phlogopite, tourmaline and chlorapatite crystals that are frequently trending along the longest axis of the scapolite crystal. Scapolite crystals also bear, generally

in their core, a few big and almost pure anorthite inclusions. BCOR 71 sample corresponds to the emblematic Pyrenean "micaceous hornfelses" (Lacroix, 1894) that result from the metamorphic evolution of evaporitic mudstones (Ravier & Thiébault, 1982).

6. BCOR 72

This white rock exhibits a layered fabric defined by phyllite and amphibole-rich beds. The bedding is also outlined by a grain-size sorting and a schistosity is observed parallel to the bedding. BCOR 72 sample is composed of an accumulation of millimetric to plurimillimetric isolated crystals, dominantly vermiculite and amphibole, all aligned in the schistosity. We performed an elemental mapping at the microstructural level by scanning electron microscopy with energy dispersive X-ray spectrometry (EDS) on this sample. As shown on Fig. 8, the mineralogical content includes, in order of abundance, isolated crystals of: gedrite, pargasite, vermiculite, aluminous enstatite, kornerupine, sapphirine, diopside, tourmaline, rutile and white mica. One millimetric kornerupine shows a subhedral shape. A very fine-grained cement composed of the same minerals and devoid of any calcite crystal can be observed locally. We observed rutile inclusions in amphibole and apatite plus rutile inclusions in kornerupine. Raman spectroscopy analyses have revealed the occurrence of anhydrite inclusions in a kornerupine crystal (Fig. 6.1).

7. BCOR 73

BCOR 73 sample was also collected in the whitest part of the outcrop. A yellowish phyllite-rich sandstone occupies two thirds of the thin section, while the remaining part is made of one centimetric subrounded greenish polymineralic clast. Under the microscope, the sandstone portion appears to be composed of angular, monomineralic grains of submillimetre to millimetre size. These grains exhibit a wide range of compositions as follows (in order of abundance): vermiculite, pargasite, clinopyroxene, scapolite, a green spinel, rutile and tourmaline. The planar minerals are roughly parallel-oriented, defining a coarse bedding. The bedding is also outlined by a grain-size sorting. There are three distinct types of vermiculite: the first one is white, the second one is yellowish with a pleochroism and the last one is characterized by an alternation of white and yellowish sheets. All the vermiculite crystals are kinked and show opened fractures and cleavages. The centimetric greenish subrounded clast derives from a scapolitized amphibolite with clinopyroxene and a few vermiculites. This mineral assemblage corresponds to a "micaceous hornfels" (Lacroix, 1894; Ravier & Thiébault, 1982), in which primary phlogopite was transformed into vermiculite. This clast is broken at its borders and feeds the sandstone with monomineralic clasts. It is also surrounded by vermiculites, oriented roughly parallel to the clast border. The lack of bedding in the part of the sample where the "micaceous hornfels" clast is observed may result from a disruption of preexisting structures when this clast was deposited.

8. LHZ 7a

This white rock is a coarse sandstone with angular fragments of white minerals up to three millimetres long visible on the hand specimen. There is a very rough bedding defined by the alignment of the largest crystals. Under the microscope, the grains are composed of monomineralic debris of dominant anthophyllite and vermiculite in a rare calcite cement. The debris are extremely angular and correspond to chips of larger crystals with no preferential orientation. Vermiculites are often kinked with opened cleavages filled in with calcite. Accessory isolated minerals include rounded grains of green aluminous spinel, sapphirine, tschermakite, tourmaline and rutile. Rare millimetre-sized sapphirine crystals have also been observed. Some sapphirines and Mg-amphiboles bear elongated rutile inclusions that align with each other. Tschermakite also often shows rutile inclusions. The sapphirine and tschermakite crystals are most often subhedral. Here again, the high concentration in anthophyllite crystals and the lack of any preferential orientation suggest an origin by accumulation through sedimentary processes.

9. Momo 2, Momo 5 & Momo 6

The centre of site 1 is marked by the presence of a layer composed of an accumulation of pluricentimetrical angular clasts of greenish to bluish rocks juxtaposed against white shining rocks (Fig. 2). Momo 2, Momo 5 and Momo 6 samples were collected from this clast accumulation. All these samples derive from "micaceous hornfelses" (Lacroix, 1894; Ravier & Thiébault, 1982). The colour changes correspond to variations in crystal concentrations as reflected by the mineralogical compositions of Momo 2, 5 and 6 samples. Momo 2 sample is very similar to BCOR 71 sample and includes, in order of abundance: scapolite, phlogopite, diopside and tourmaline. The scapolite crystals bear small inclusions of phlogopite, tourmaline and apatite that align with the longest axis of their host. Some scapolite crystals also bear large anorthite cores. Momo 6 sample includes: dominant diopside and phlogopite, scapolite, anorthite and zoisite. Thus, it equates to Momo 2 sample. Momo 5 sample is made up of: scapolite, diopside, anorthite, phlogopite, potassian hastingsite, tourmaline and calcite. Phlogopite content is lower than in BCOR 71 and Momo 2 sample, and anorthite crystals are more abundant and not necessarily included in scapolites. Momo 5 corresponds to an intermediate facies between the "micaceous hornfels" and the surrounding marbles, which according to Ravier & Thiébault (1982) results from the metamorphism of alternating argillites and dolomitic argillites of Triassic to Lower Liassic ages.

10. LHZ 114a

This sample comes from a contact zone with the Lherz body. Here, decimetrical clasts of ophicalcites are embedded within greenish to bluish coarse sandstones. The thin section was prepared at the edge of the ultramafic clast and is composed of a part of the peridotite and of the surrounding sandstone. The ultramafic rock is a partly serpentinized lherzolite showing a mesh texture invaded by a network of orthogonal calcitic veins. The sandstone is cemented by calcite. It includes a great variety of angular fractured millimetric to submillimetric monomineralic grains including: dominant vermiculite, gedrite, pargasite, enstatite, diopside, serpentine, sapphirine and aluminous spinel. No bedding is observed at the scale of the thin section.

11. BCOR 67b

This white rock is comparable to LHZ 7a, Momo 2a and Momo 2b sapphirine-bearing sandstones described above. Under the microscope, it appears as a microbreccia made up of rare and extremely fractured millimetre-sized clasts in a dominant isogranular sparitic cement. Most of the clasts are monomineralic and include, in order of abundance: vermiculite, smectite, aluminous spinel, sapphirine, rutile and chlorapatite. The aluminous spinel show corrosion gulfs filled by calcite. Unlike the clasts, the calcitic cement is not fractured. No bedding is observed at the scale of the thin section.

12. BCOR 68a

BCOR 68a sample is another example of sapphirine-bearing sandstone. This white and shiny phyllite-rich sample bears numerous plurimillimetric bluish clasts. Under the microscope, it appears as a microbreccia made up of major monomineralic and minor polymineralic clasts in an isogranular sparitic cement. The clasts are highly fractured in contrast with euhedral and homogeneous calcite crystals. The monomineralic debris include: vermiculite, smectite, anthophyllite-gedrite, sapphirine and rutile. Vermiculite is frequently kinked, with opened fractures and ponytail edges. The bluish plurimillimetric clasts distinguishable with the naked eye are sapphirine crystals. Most often, the sapphirine crystals show subhedral shapes. They are often surrounded by fibrous smectite rims. One centimetric and highly fractured anthophyllite crystal is also present in the thin section. The fractures of the clasts are filled by calcite. Polymineralic clasts include different types of mineral intergrowths of sapphirine and anthophyllite, anthophyllite and vermiculite, as well as sapphirine, anthophyllite and vermiculite. Sapphirine crystals display apatite inclusions extremely rich in Cl. We also observed aligned inclusion trails of rutile in sapphirine and Mg-amphibole crystals.

13. BCOR 68b

This rock is extremely similar to BCOR 68a sample. An important feature of this sample is the presence of chlorapatite inclusions extremely rich in Cl in the sapphirine and Mg-amphibole crystals.

14. NR 94

This sample was collected five metres away from the massive lherzolite during earlier field work by one of us (P. Monchoux) and was studied during two unpublished master thesis at the University of Toulouse by N. Ribot (1993-1994) and F. Foucard (1996-1997). The macroscopic observation shows coarse centimetric yellowish to reddish layers alternating with greyish to bluish layers. The yellowish to reddish layers display abundant blue centimetric crystals of spinel, within abundant phyllites and oxides. The large spinels reach a maximum size of 2 cm. The finer levels contain the same blue spinels, with a millimetric size. Under the microscope, the sample appears as a layered microbreccia, cemented by calcite. Both layers are made up of monomineralic clasts, in various proportions, including: aluminous spinel, aluminous enstatite, pargasite, vermiculite, zircon, rutile, apatite and oxides. Some amphiboles reach a maximum size of 5 mm. The yellowish to reddish layers are richer in vermiculite and large spinels whereas the greyish layers are richer in amphiboles. The calcite is mostly fine-grained, but larger euhedral crystals are also observed. Vermiculite is either brown or white, always kinked with open cleavages. Except for vermiculite, the monomineralic clasts are invariably broken, but the debris underwent minor reworking since it is possible to restore the initial subhedral shape of several crystals of spinel and amphibole. The enstatite crystals of this sample include a great diversity of inclusions, as follows: anhydrite inclusions enriched in Sr, chlorapatite inclusions enriched in F and sometimes coalescing with anhydrite inclusions, clinochlore and zircon inclusions. Chlorapatite and zircon inclusions are also present in pargasite crystals.

SM3: BSE images of some rutile grains used for U-Pb dating.

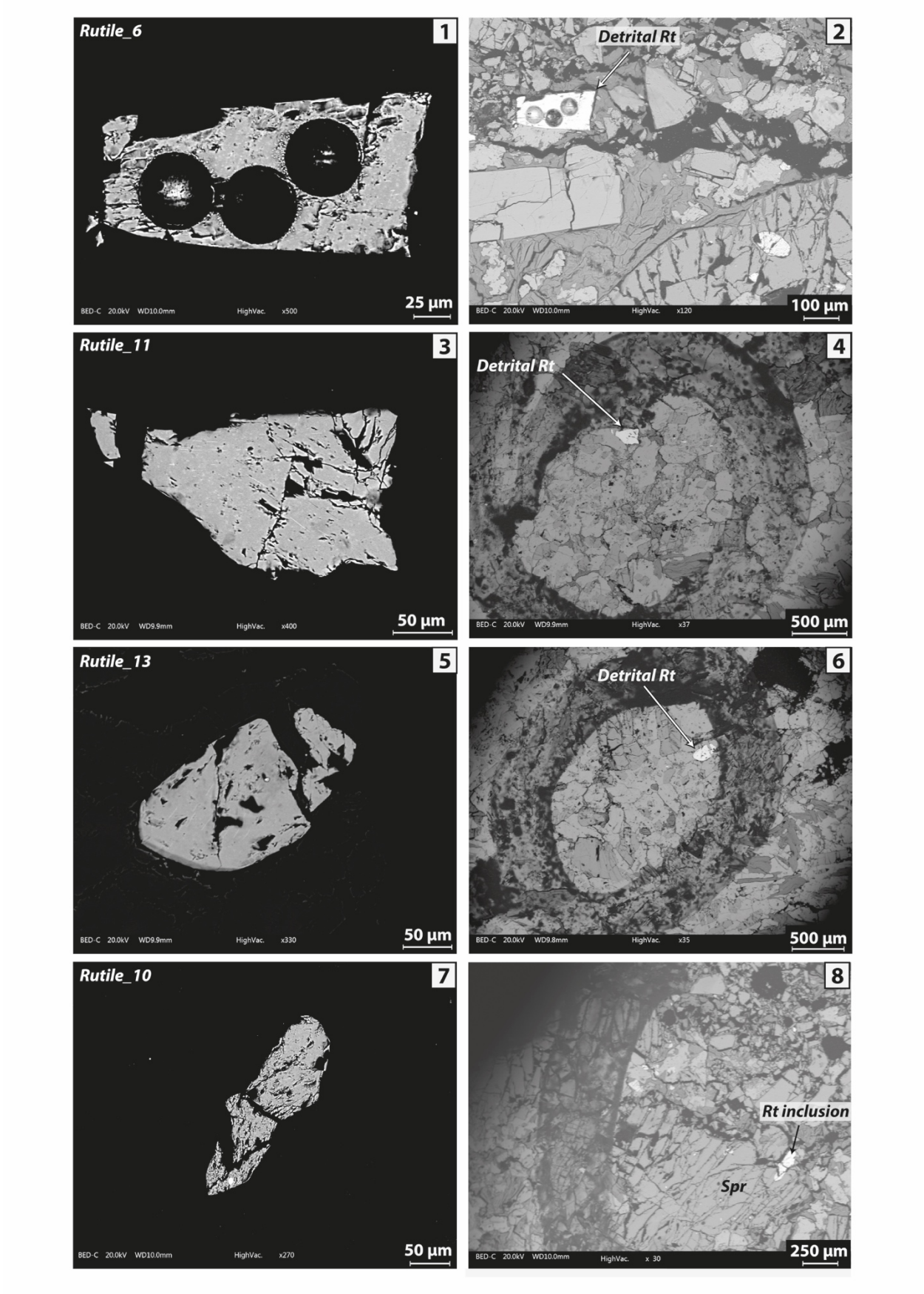

1, 3, 5, 7: close-up views of the rutile grains. 2,4,6,8: immediate surroundings of the rutile grains in the thin section.